Nanotechnology **20** (2009) 015303 (5pp) doi:10.1088/0957-4484/20/1/015303

Geometry transformation and alterations of periodically patterned Si nanotemplates by dry oxidation

Jeongwon Park, Li-Han Chen, Daehoon Hong, Chulmin Choi, Mariana Loya, Karla Brammer, Prab Bandaru and Sungho Jin

Materials Science and Engineering Program, Mechanical and Aerospace Engineering, University of California, San Diego, La Jolla, CA 92093-0411, USA

E-mail: jin@ucsd.edu

Received 22 July 2008, in final form 20 October 2008
Published 5 December 2008
Online at stacks.iop.org/Nano/20/015303

Abstract
We report on the size-dependent transformation and geometrical modifications of periodically patterned Si templates by a combination of dry oxidation and chemical etching. Deep ultraviolet lithography patterned circular holes with diameters varying between 190 nm and 1 μm on Si wafers were oxidized at 1000 °C using dry oxygen for various durations, with selected samples chemically etched for oxide removal for additional alterations. An interesting phenomenon of a circular-to-square shape transformation of the holes was observed, which was particularly pronounced in the sub-200 nm regime. We tentatively attribute the change to the surface energy and geometry constraints in nanoscale patterns.

(Some figures in this article are in colour only in the electronic version)

1. Introduction

Templated silicon nanostructures can be useful for nano-imprint lithography, large scale fabrication of component features in micro/nano-electromechanical systems (MEMS, NEMS), microfluidics, photonic crystal circuits, and for designed cell growth in biological applications [1–4]. Silicon nanotemplates are generally fabricated by lithographic techniques using electron beams [5, 6], deep ultraviolet (DUV) processes, x-rays [7], and focused ion beams [8]. It would be desirable to find a way of utilizing a fixed nanotemplate and find a simple means of inducing different geometries. Here we demonstrate that a combination of thermal oxidation and chemical etching of DUV-patterned Si nanostructures can induce a variety of shape changes which can be used to tailor individual nanotemplates with approximately 100 nm features. While Si oxidation has been extensively studied under a variety of process conditions [9–18], as in the Deal–Grove model [10], the corresponding effects at the nanoscale have not been well investigated. For example, we have observed in the oxidation of sub-micron silicon features, significant geometry changes, the most fascinating of which was a circle-to-square pattern transformation. This letter reports on these results on induced dimensional changes of nanotemplates and attempts to provide some interpretations.

2. Experimental details

2.1. Fabrication process with deep UV lithography

A typical DUV process for fabrication of the initial Si nanotemplates is schematically illustrated in figure 1. The nanotemplates were fabricated on (100) silicon wafers patterned with 193 nm DUV lithography and a reactive-ion-etch (RIE) process with oxide hard-mask to achieve the desired fine-geometries as described below. Approximately 100 nm thick SiO_2 was deposited on 300 mm diameter silicon wafers in an Applied Materials 5000 plasma enhanced chemical vapor deposition (PE-CVD) system using tetraethoxysilane (TEOS) chemistry. A UV-sensitive high resolution photoresist was then spin coated on the silicon wafers (see figures 1(a) and (b)). On top of the resist, an anti-reflective (AR) coating was applied to eliminate standing waves in the photoresist (figure 1(c)). The DUV lithography to create a pattern of holes was performed on an ASML/SVGL Micrascan 193 nm step-and-scan lithography system (figure 1(d)). After lithography,

 © 2009 IOP Publishing Ltd Printed in the UK

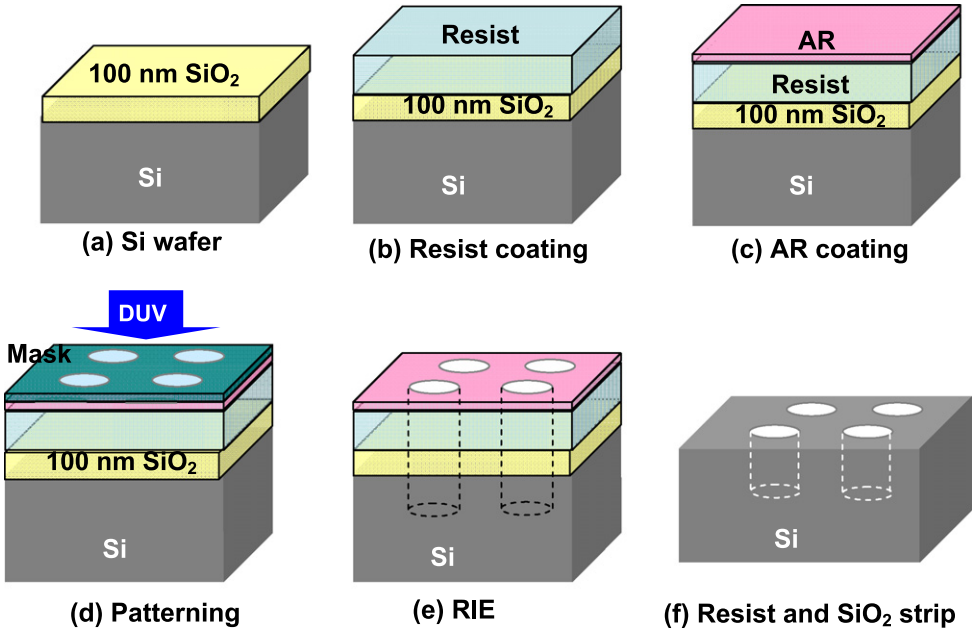

Figure 1. Schematic illustration of the Si nanotemplate fabrication process using DUV lithography.

the resist was developed. A hard-mask of 100 nm silicon oxide was used to transfer this fine lithographic definition by RIE steps first into the hard-mask and then into the silicon substrate with high fidelity (figure 1(e)). The SiO_2 was etched with fluorine-based chemistry in an Applied Materials Centura 5200 etcher and the silicon was etched with chlorine-based chemistry in a LAM Rainbow 9400PTX etcher (figure 1(f)).

2.2. Dry oxidation and wet etching

Samples were precleaned using standard Radio Corporation of America (RCA) cleaning sequence [19, 20], followed by a dip in buffered oxide etchant (BOE) to remove oxide. To intentionally reduce the nanotemplate hole dimension, some samples were placed in a conventional resistive heating furnace and oxidized in pure O_2 (99%) at 1000 °C, with optional chemical etching of the oxide layer by using BOE solution to further enlarge the hole diameter. The temperature in the oxidation tube was controlled by automated profiling.

2.3. Sample characterization

The extent of oxidation, as reflected in the shape and size of the modified patterns checked by using a field emission scanning electron microscope (FESEM: Phillips XL30 ESEM). A focused ion beam (FIB: Zeiss Crossbeam 1540X: 30 keV) apparatus used for cross-sectional profile analysis. The cross-sectioning of the DUV Si samples by FIB milling was carried out using a current of 200–500 pA and the imaging was done using a current of 10–50 pA.

3. Results and discussion

Shown in figure 2 is the progressive change in the nanotemplate hole geometry by the 1000 °C oxidation. The virgin sample exhibits 190 and 1000 nm diameter circular silicon hole pattern with 970 nm depth (figures 2(a) and (d)), after 45 min oxidation (figures 2(b) and (e)) and after 180 min of oxygen exposure (figures 2(c) and (f)). The hole geometry is significantly altered in small diameter samples. It was seen, in this specific case, that the oxidation reduces the diameter (or the smallest dimension of the hole) from ∼190 nm to 146 ± 3 nm after 45 min (figure 2(b)) and 119 ± 2 nm after 180 min (figure 2(c)), corresponding to the diameter change due to oxidation of 44 ± 3 nm and 71 ± 2 nm, respectively. We see clearly from higher magnification imaging (insets to figure 2) a circular-to-square geometry transformation facilitated by the dry oxidation process. In figures 2(b) and (c), the surfaces of square holes consist of {100} orientations. The circular-to-square geometry transformation is particularly obvious for smaller diameter (<200 nm) circular geometries.

When the grown Si oxide layer is removed through selective chemical etching using HF-based solution, the resultant Si hole diameter becomes much larger (∼230–350 nm depending on the extent of the oxidation treatment) than the original 190 nm diameter, as the growth/penetration of silicon oxide occurs 54% above and 46% below the original silicon surface [9, 10]. Additionally, the square holes revert to a circular shape. The above processes, based on oxidation and chemical etching, provide additional means of adjusting the nanotemplate dimensions to any specific size scale within the broad regime of ∼120–350 nm, and is convenient for preparation of a variety of Si or SiO_2 nano-imprint inverse molds, and daughter molds with different geometries (such as a pillar array of thermoplastic or elastomeric polymer materials) from a fixed geometry Si nanotemplate. Such variations could also be useful for construction of photonic crystals with varying frequency responses [21].

We used a focused ion beam (FIB) to delineate the cross-sectional shape of the holes in the nanotemplates, as shown

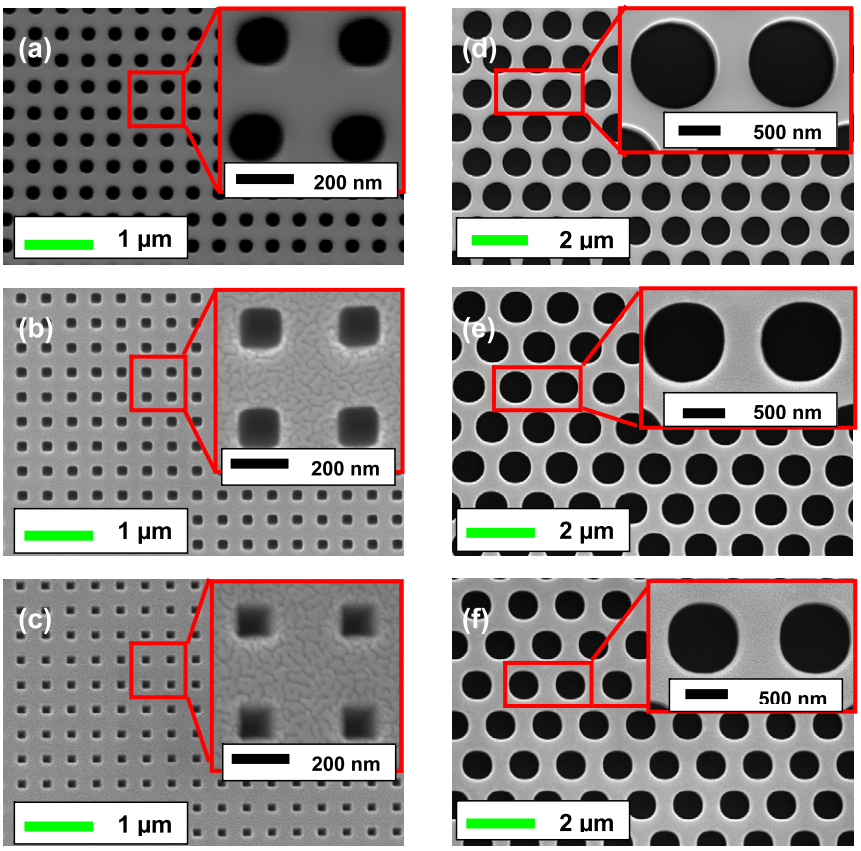

Figure 2. SEM images of square hole versus round hole geometry formed in oxidized Si nanotemplates for small (190 nm) ((a)–(c)) versus large (1000 nm) starting Si hole diameter ((d)–(f)). (a) and (d) As-DUV-patterned round hole array, (b) and (e) square hole array after dry oxidation at 1000 °C for 45 min, (c) and (f) after additional dry oxidation at 1000 °C for 180 min. The square hole face orientation are {100} orientations. The oxidized surface (figures 1(b) and (c)) was coated with gold (∼2 nm thick) for easier SEM examination, which causes the granular pattern on the sample surface.

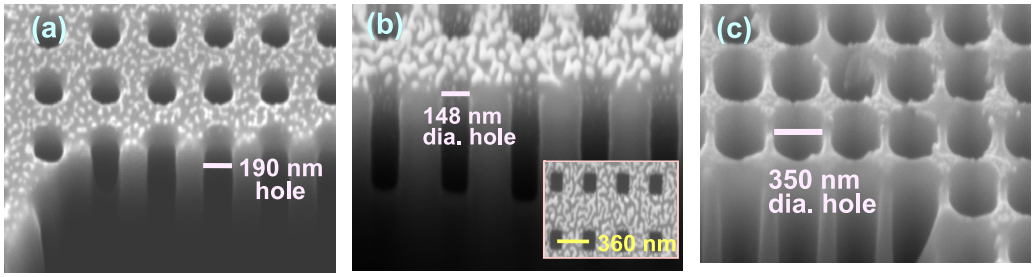

Figure 3. Focused ion beam cross-section of DUV silicon patterns showing the controlled variation of Si hole diameter by processing. (a) As-DUV patterned, (b) oxidized at 1000 °C/45 min (the inset depicts the SEM image of oxidation-induced square shape hole geometry which appears elongated due to sample tilting for SEM), (c) further oxidized (1000 °C/180 min) + oxide removed by chemical etching. The white spots are gold coating added for reduced charging effect during SEM imaging.

in figure 3. It is seen that the hole diameter is reasonably uniform along the depth of the holes. The initial DUV pattern exhibits an average diameter of ∼190 nm (figure 3(a)), which is substantially reduced to ∼148 nm after the 45 min oxidation, figure 3(b). (The inset depicts the top view SEM image of oxidation-induced square shape hole geometry which appears elongated due to sample tilting for SEM imaging.) After additional oxidation (180 min total) followed by chemical etch removal of the oxide layer using BOE solution of 6 parts 40% NH_4F and 1 part 49% HF, the hole diameter is increased significantly to ∼350 nm diameter. These results indicate the versatility of the processing steps utilized here for creation of any desired hole array dimensions, for example, to fabricate nano-imprint stamps with a series of dimensions from the same basic Si nanotemplate mold.

Figure 4(a) shows the extent of oxidation with different initial diameters ranging from 190 nm to 1 μm. It was seen that the incremental oxidation in terms of percent decrease in diameter is more pronounced for smaller diameter holes, as shown in figure 4(b). The relative diameter change saturates

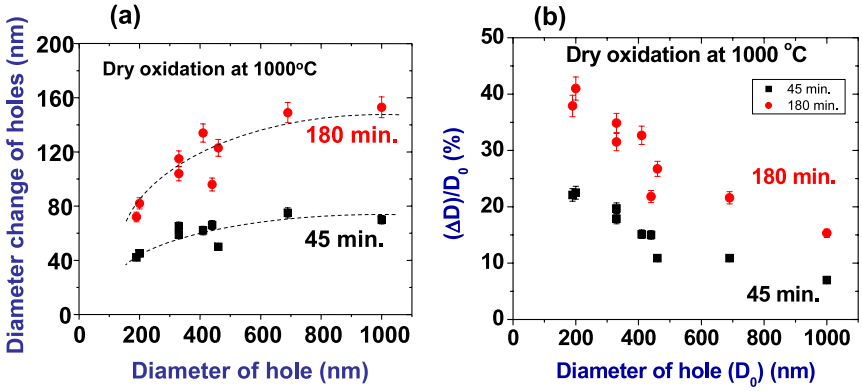

Figure 4. (a) Diameter reduction of holes with different starting diameters from 190 nm to 1 μm after dry oxidation at 1000 °C for 45 and 180 min. The average diameter reduction is indicated by dotted curves. (b) Relative diameter change after dry oxidation with different starting diameters.

presumably due to the increased difficulty of Si diffusion to the surface through the thickened SiO_2 when the diameter of the hole is larger than 690 nm. While it may not be quite accurate for the nanopatterned structure on the silicon surface, the expected oxide thickness was nevertheless roughly calculated from oxidation of plane silicon for dry oxygen at 1000 °C based on Deal–Grove model equation [10]

$$X_{ox}^2 + 0.165X_{ox} = 0.0117(t + 0.37). \quad (1)$$

Here X_{ox} is the oxide thickness (μm), and t is the oxidation time (hour). The theoretically calculated values of the diameter change from the Deal–Grove model [10] after dry oxidation at 1000 °C are 61 nm and 146 nm for 45 min and for 180 min, respectively. The hole diameter changes after oxidation are summarized in table 1. The measured diameter changes are consistently smaller than those of theoretical values in smaller diameter holes, but are well within the range expected by the Deal–Grove model when the diameter of the hole is larger than 690 nm. Generally, the oxide thickness on the cavity wall is expected to be less than the case of an exposed planar surface due to the gas flow-limiting geometry [17].

We postulate a very simple model to understand the circular to square hole shape transformation, based on surface energy and geometry considerations. In a circular hole, the surface energy (γ) is approximated by an average over various possible configurations of the planes, i.e., $\sim\frac{1}{3}\{\gamma_{(100)} + \gamma_{(110)} + \gamma_{(111)}\}$, which is around 1.46 J m^{-2} [22]. However, the sides of the square hole are found to be parallel to the (100) planes, where $\gamma_{(100)}$ is 1.34 J m^{-2}. Then, the average surface energy (SE) per unit depth of the circular hole with a radius r is [$2\pi r$ (circumference of a circle) $\times 1.46$ J m^{-2}] $= 9.17r$ J m^{-1}, while that of the square hole with an edge length of $\sqrt{2}r$ fitting inside the circular hole is [$4 \times \sqrt{2}r \times 1.34$ J m^{-2}] $= 7.58r$ J m^{-1}. From this, it is clear that the square shape is energetically favored with lower surface energy, which could tentatively explain the transformation. It is important to note that the above argument constitutes a crude approximation as it predicts that the energy is lowered by 17% [$(SE_{circle} - SE_{sqare})/SE_{circle} \times 100\%$] on circular $\rightarrow$ square transformation due to the oxidation. Further refinements such as (1) more accurate determination of the oxidation as a function of initial radius and wafer orientation, (2) modeling the gas kinetics, and (3) stress-dependent oxidation [12, 15–17], will enable to pin down the shape transformation mechanism(s) in these nanoscale patterns. The oxygen flow could be especially important as fluid capillary forces (scaling as $1/r$) dominate in smaller diameter holes.

Table 1. Summary of diameter changes after dry oxidation.

Initial hole diameter (nm)	Hole diameter changes (nm)	
	After 45 min	After 180 min
190	44	72
330	59	115
440	66	96
690	75	149
1000	70	153

Previous studies of Si oxidation have shown that the oxidation rate depends on a number of parameters such as the crystal orientation of the silicon substrate [11–14], stress [12, 15–17], and oxygen diffusivity [18]. The relative oxidation rate of (100) Si surfaces is generally slower than other planes for both dry and wet oxidation due to the lower surface density of Si atoms and the smaller number of available Si–Si bonds [13, 14]. This differential oxidation rate between (100) and other planes, e.g, (110), (111), etc, would also produce a circular-to-square geometry transformation observed in our samples. Other factors that might be considered for the circular-to-square geometry transformation is the influence of stress [12, 15–17] at the interface between Si and SiO_2, and that of oxygen diffusivity [18]. However, the exact mechanism of the observed circular-to-square geometry transformation is unknown at the moment and further in-depth studies are in progress to clearly understand the mechanism.

4. Summary

In summary, we have demonstrated that the nanotemplate geometry and dimensions in DUV lithography patterned Si samples can be tuned by oxidative and etching processes

which enable modification and creation of nanotemplate dimensions with any specific size scale within the broad regime of ∼120–350 nm. Such a capability is convenient for preparation of a variety of Si or SiO_2 nano-imprint stamps, inverse molds, and daughter molds from a fixed geometry Si nanotemplate. Such adjustable geometry can enable preparations of various nanostructures for physical studies and technical applications, for example, fabrication of versatile nano-imprint molds, MEMS/NEMS devices, photonic crystals, and other applications. It was also found that a circular-to-square shape change occurs for smaller template hole diameters (near ∼200 nm), but the effect is negligible for larger initial hole diameters. We propose a tentative surface energy model to explain the transformation.

Acknowledgments

This research was supported by NSF-NIRT under Grant No. DMI-0303790, University of California Discovery Fund under Grant No. ele05-10241/Jin, CNMT Grant No. 05K1501-01210 under the 21st Century Frontier R&D Programs, Ministry of Science and Technology, Korea, and Iwama Endowed fund. The joint support by US Air Force Office of Scientific Research and Ministry of Science and Technology of Korea under Nano/BioO/Info Technology (NBIT) Symbiosis Program is also acknowledged.

References

[1] DiVentra M, Evoy S and Heflin J R 2004 *Introduction to Nanoscale Science and Technology* (Dordrecht: Kluwer Academic)
[2] Wanga B, Zhaoa W, Chenb A and Chuaa S J 2006 *J. Cryst. Growth* **288** 200
[3] Marsal L F, Trifonov T, Rodriguez A, Pallares J and Alcubilla R 2003 *Physica* E **16** 580
[4] Bhushan B 2007 *Handbook of Nanotechnology* 2nd edn (Berlin: Springer)
[5] Storm A J, Chen J H, Ling X S, Zandbergen H W and Dekker C 2005 *J. Appl. Phys.* **98** 014307
[6] Madou M J 2002 *Fundamentals of Microfabrication: The Science of Miniaturization* 2nd edn (Boca Raton, FL: CRC Press)
[7] Silverman J P 1998 *J. Vac. Sci. Technol.* B **16** 3137
[8] Arshaka K, Mihovb M, Nakaharab S, Arshakc A and McDonaghd D 2004 *Superlatt. Microstruct.* **36** 335
[9] Blanc J 1978 *Appl. Phys. Lett.* **33** 424
[10] Deal B E and Grove A S 1965 *J. Appl. Phys.* **36** 3770
[11] Raider S I and Forget L E 1980 *J. Electrochem. Soc.* **127** 1783
[12] Uematsu M, Kageshima H and Shiraishi K 2000 *Japan. J. Appl. Phys.* **39** 1135
[13] Ngau J L, Griffin P B and Plummer J D 2002 *J. Electrochem. Soc.* **149** F98
[14] Ligenza J R 1961 *J. Phys. Chem.* **65** 2011
[15] Kao D B, McVittie J P, Nix W D and Saraswat K C 1987 *IEEE Trans. Electron Devices* **34** 1008
[16] Heidemeyer H, Single C, Zhou F, Prins F E, Kern D P and Plies E 2000 *J. Appl. Phys.* **87** 4580
[17] Kao D B, McVittie J P, Nix W D and Saraswat K C 1988 *IEEE Trans. Electron Devices* **35** 25
[18] Liu H I, Biegelsen D K, Ponce F A, Johnson N M and Pease R F W 1994 *Appl. Phys. Lett.* **64** 1383
[19] Kern W and Puotinen D A 1970 *RCA Rev.* 187
[20] Kern W 1993 *Handbook of Semiconductor Wafer Cleaning Technology* (Park Ridge, NJ: Noyes Publications)
[21] Johnson S G and Joannopoulos J D 2002 *Photonic Crystals: The Road from Theory to Practice* (Berlin: Springer)
[22] Messmer C and Bilello J C 1981 *J. Appl. Phys.* **52** 4623